Four-body continuum-discretized coupled-channels calculations using a transformed harmonic oscillator basis

M. Rodríguez-Gallardo[1,2,3], J. M. Arias[2], J. Gómez-Camacho[2],
R. C. Johnson[3], A. M. Moro[2], I. J. Thompson[3,4], and J. A. Tostevin[3]
[1] *Centro de Física Nuclear, Universidade de Lisboa,*
Av. Prof. Gama Pinto n°2, 1649-003 Lisboa, Portugal
[2] *Departamento de Física Atómica, Molecular y Nuclear,*
Universidad de Sevilla, Apartado 1065, 41080 Sevilla, Spain
[3] *Department of Physics, University of Surrey, Guildford GU2 7XH, United Kingdom and*
[4] *Lawrence Livermore National Laboratory, PO Box 808, L-414, Livermore, CA 94551, USA*
(Dated: July 2, 2008)

The scattering of a weakly bound three-body system by a target is discussed. A transformed harmonic oscillator basis is used to provide an appropriate discrete and finite basis for treating the continuum part of the spectrum of the projectile. The continuum-discretized coupled-channels framework is used for the scattering calculations. The formalism is applied to different reactions, ^{6}He+^{12}C at 229.8 MeV, ^{6}He+^{64}Zn at 10 and 13.6 MeV, and ^{6}He+^{208}Pb at 22 MeV, induced by the Borromean nucleus ^{6}He. Both the Coulomb and nuclear interactions with a target are taken into account.

PACS numbers: 21.45.+v,21.10.-k,27.20.+n,24.10.-i,24.10.Eq,25.60.-t,25.60.Bx,03.65.Ca

I. INTRODUCTION

The development of radioactive nuclear beam facilities has allowed the study of nuclei far from the line of stability, bringing to the fore new nuclear structure problems. A significant topic in recent years has been the study of halo nuclei [1, 2, 3]. These are weakly bound, spatially extended systems, typically comprising a core and one or two valence nucleons. Particularly interesting examples of such systems are Borromean nuclei, i.e., three-body composite systems with no binary bound states. These nuclei have attracted special attention because their loosely bound nature reflects a delicate interplay between two- and three-body forces, constituting a challenge to existing theories, and a motivation for the development of new ones. The detailed structure of the continuum spectrum of these systems is still not fully understood, partially due to the ambiguities associated with the underlying forces between the constituents. Due to their low binding energy, halo nuclei are easily broken up in the nuclear and Coulomb field of the target nucleus. Therefore few-body reaction theories, developed to extract reliable information from experimental data of reactions involving loosely bound systems, have to include, as an essential ingredient, a realistic description of coupling to the continuum part of the spectrum.

From the theoretical point of view, the treatment of reactions involving loosely bound systems must deal with the complication that these continuum breakup states are not square-normalizable. A convenient method to circumvent this problem is to replace the states in the continuum by a finite set of normalized states, thus providing a discrete basis that, hopefully, can be truncated to a small number of states and yet provide a reliable description of the continuum. Several prescriptions to construct such a discrete basis have been proposed. For two-body composite systems, where the continuum states are easily calculated, one can use a discretization procedure in which the continuum spectrum is truncated at a maximum excitation energy and divided into energy intervals. For each interval, or bin, a normalizable state is constructed by superposition of scattering states within that bin interval. The method, normally used in the continuum-discretized coupled-channels (CDCC) framework [4, 5], has been very useful in the description of elastic and breakup observables in reactions involving weakly bound two-body projectiles.

An alternative to the binning procedure is to represent the continuum spectrum by the eigenstates of the internal Hamiltonian in a basis of square integrable (or L^2) functions, such as Laguerre [6, 7, 8], Gaussian [9, 10] or Sturmian [11, 12, 13, 14] functions. In practice, the diagonalization is performed in a finite (truncated) set of states and the resulting eigenstates, also known as *pseudo-states* (PS), are regarded as a finite and discrete representation of the spectrum of the system. The pseudo-states are then used within a coupled-channels calculation in the same way as the continuum bins.

The PS method has the appealing feature of being readily applicable also to describe the spectrum of three-body systems, in which case the Hamiltonian is diagonalized in a complete set of square-integrable functions for the three-body Hilbert space. Several applications of this method can be found in the literature, for both structure [15] and reaction problems [16]. In the latter case, the method is an extension of the CDCC formalism to reactions with three-body projectiles, using a pseudo-state model for the continuum.

One such PS method proposed recently is the Transformed Harmonic Oscillator (THO) method [17, 18]. Given the ground-state wave function of the system, the THO method performs a Local Scale Transformation

(LST) [19] that converts the bound ground-state wave function of the system into the ground-state wave function of a Harmonic Oscillator (HO). Once the LST is obtained, the HO basis can be transformed, by the inverse LST, to a discrete basis in the physical space. The THO basis functions are not eigenfunctions of the Hamiltonian (except for the ground state) but the Hamiltonian can be diagonalized in an appropriate truncated basis to produce approximate eigenvalues and eigenfunctions. This method has been shown to be useful for describing the two-body continuum in both structure [17, 18, 20] and scattering [21, 22, 23] problems. In a recent work [24] the THO method was generalized to describe continuum states of three-body systems, based on expansion in Hyperspherical Harmonics (HH) [25]. In particular the method was applied to the Borromean nucleus ^{6}He, for which several strength functions, including the dipole and quadrupole Coulomb transition strengths, were calculated. These observables are found to converge quickly with respect to the number of THO basis states included. Furthermore, the calculated strength distributions are in very good agreement with those obtained using three-body scattering wave functions [26].

Most of our knowledge of ^{6}He comes from the analysis of reactions where secondary beams collide with stable nuclei. These experiments have been performed with both light [27, 28] and heavy targets [29, 30, 31, 32, 33], and at low and high energies, providing a body of data which can be used to benchmark reaction and structure models. The theoretical understanding of reactions involving a three-body projectile, such as ^{6}He, is a complicated task because it requires the solution of a four-body scattering problem. At high energies, a variety of approximations have been used such as semiclassical approximations [34, 35, 36], *frozen halo* or adiabatic approximations [37, 38], Multiple Scattering expansions [39, 40, 41], four-body DWBA [42, 43], among others. However, at energies of a few MeV per nucleon, some of these approximations are not justified. Then the use of the CDCC method is an alternative to solve these problems. For a four-body problem (three-body projectile) this method has already been applied using a PS basis based on Gaussian functions. The scattering of ^{6}He by ^{12}C [16] and ^{209}Bi [44] have been studied. In both cases a good agreement was obtained with the experimental data of Refs. [45, 46] and [31], respectively.

In this work, we study the scattering of a three-body projectile by a target using the CDCC formalism. The novel feature of the present approach is the use of the THO PS basis to represent the states of the projectile. These states are then used to generate the projectile-target coupling potentials that enter the system of coupled equations. Furthermore, we have developed a new procedure to calculate these coupling potentials making use of an expansion of the wave functions of the projectile internal states in a HH basis.

This paper is structured as follows. In Section II the three-body discretization method is presented. In Section III the multipole expansion of the interaction potential between the projectile and the target is addressed. In Section IV we describe the three-body model for the Borromean nucleus ^{6}He. In Section V we apply the formalism to the reactions ^{6}He+^{12}C at $E_{\rm lab}$=229.8 MeV, ^{6}He+^{64}Zn at $E_{\rm lab}$=13.6 and 10 MeV, and ^{6}He+^{208}Pb at $E_{\rm lab}$=22 MeV. Finally, Section VI summarizes and draws conclusions.

II. THREE-BODY CONTINUUM DISCRETIZATION METHOD

The THO discretization method applied to a three-body system is described in detail in Ref. [24]. For completeness, in this Section we outline the main features of the formalism. In the three-body case, it is convenient to work with the hyperspherical coordinates $\{\rho, \alpha, \widehat{x}, \widehat{y}\}$. They are obtained from the Jacobi coordinates $\{\boldsymbol{x}, \boldsymbol{y}\}$ that are illustrated in Fig. 1. The variable $\boldsymbol{x}$ is proportional to the relative coordinate between two of the particles, with a scaling factor depending on their masses [20] and $\boldsymbol{y}$ is proportional to the coordinate from the center of mass of these two particles to the third particle, again with a scaling factor depending on their masses. From these coordinates, the hyperradius (ρ) and the hyperangle (α) are defined as $\rho = \sqrt{x^2+y^2}$ and $\tan\alpha = x/y$. Obviously there are three different Jacobi sets but ρ is the same for all of them.

For a three-body system the discretization method has two parts. First, the wave functions of the system are expanded in Hyperspherical Harmonics (HH) [25]. We define states of good total angular momentum as

$$\begin{aligned}\mathcal{Y}_{\beta j\mu}(\Omega) &= \sum_{\nu\iota}\langle j_{ab}\nu I\iota|j\mu\rangle\chi^{\iota}_{I} \\ &\times \sum_{m_l\sigma}\langle lm_l S_x\sigma|j_{ab}\nu\rangle\Upsilon^{l_xl_y}_{Klm_l}(\Omega)\chi^{\sigma}_{S_x}, \end{aligned} \quad (1)$$

where $\Upsilon^{l_xl_y}_{Klm}(\Omega)$ are the hyperspherical harmonics that depend on the angular variables $\Omega \equiv \{\alpha, \widehat{x}, \widehat{y}\}$, $\chi^{\sigma}_{S_x}$ is the spin wave function of the two particles related by the coordinate $\boldsymbol{x}$, and χ^{ι}_{I} is the spin function of the third particle. Each component of the wavefunction (or channel) is defined by the set of quantum numbers $\beta \equiv \{K, l_x, l_y, l, S_x, j_{ab}\}$. Here, K is the hypermomentum, l_x and l_y are the orbital angular momenta associated with the Jacobi coordinates $\boldsymbol{x}$ and $\boldsymbol{y}$, $\boldsymbol{l} = \boldsymbol{l}_x + \boldsymbol{l}_y$ is the total orbital angular momentum, S_x is the spin of the particles related by the coordinate $\boldsymbol{x}$, and $\boldsymbol{j}_{ab} = \boldsymbol{l} + \boldsymbol{S}_x$. Finally, $\boldsymbol{j} = \boldsymbol{j}_{ab} + \boldsymbol{I}$ is the total angular momentum, with I the spin of the third particle, which we assume fixed. The physical states of the system can now be expressed as a linear combination of the states given by Eq. (1) as

$$\psi_{j\mu}(\rho, \Omega) = \sum_{\beta} R_{\beta j}(\rho)\mathcal{Y}_{\beta j\mu}(\Omega), \quad (2)$$

where $\{R_{\beta j}\}$ are the hyperradial wave functions.

Secondly, the THO method is used to obtain the functions $R_{\beta j}(\rho)$. Writing the ground-state wave function in the form of Eq. (2), the equation that defines the LST for each channel β is

$$|N_{B\beta}|^2 \int_0^\rho d\rho' \rho'^5 |R_{B\beta}(\rho')|^2 = \int_0^s ds' s'^5 |R^{HO}_{0K}(s')|^2, \quad (3)$$

where $R_{B\beta}(\rho)$ is the bound ground-state hyperradial wave function for the channel β, with $N_{B\beta}$ the normalization factor, and $R^{HO}_{0K}(s)$ is the ground-state hyperradial wave function of the HO for the hypermomentum K, that is already normalized. Finally, the THO basis is constructed for each channel by applying the LST, $s_\beta(\rho)$, to the HO basis

$$R^{THO}_{i\beta}(\rho) = \frac{\mathcal{N}_{iK}}{\mathcal{N}_{0K}} N_{B\beta} R_{B\beta}(\rho) L_i^{K+2}(s_\beta(\rho)^2), \quad (4)$$

$$\psi^{THO}_{i\beta j\mu}(\rho, \Omega) = R^{THO}_{i\beta}(\rho) \mathcal{Y}_{\beta j\mu}(\Omega) \quad (5)$$

where the $L_i^\lambda(t)$ are generalized Laguerre polynomials and $\mathcal{N}_{iK}$ is the normalization constant of the HO basis. Here the index i denotes the number of hyperradial excitations. Note that as i increases, the functions $R^{THO}_{i\beta}(\rho)$ become more oscillatory and explore larger distances.

For channels with quantum numbers that do not contribute to the ground-state wave function, the (ground state) channel with the closest quantum labels to the channel of interest is used to construct the LST. One important point concerns the label K which governs the ρ^K behavior of the hyperradial wave function close to the origin. To guarantee the correct behavior of the wavefunction, we select a channel from the ground-state wave function with the same K. If this is not possible, a channel with $K-1$ is used and the corresponding hyperradial wave function is then multiplied by ρ.

The required discrete eigenstates are now calculated by diagonalizing the three-body Hamiltonian of the projectile in a finite THO basis up to n_b hyperradial excitations in each channel,

$$\phi^{THO}_{njJ\mu}(\boldsymbol{x}, \boldsymbol{y}) = \sum_\beta \sum_{i=0}^{n_b} C_n^{i\beta j} \psi^{THO}_{i\beta j\mu}(\rho, \Omega), \quad (6)$$

where n labels the eigenstates for a given angular momentum j and ε_{nj} will be the associated energy. Replacing in this expression the functions $\psi^{THO}_{i\beta j\mu}(\rho, \Omega)$ by their explicit expansion in terms of the HH, Eq. (5), and performing the sum in the index i for $i = 0, \ldots, n_b$, we can express the PS basis states as

$$\phi^{THO}_{njJ\mu}(\boldsymbol{x}, \boldsymbol{y}) = \sum_\beta R^{THO}_{n\beta j}(\rho) \mathcal{Y}_{\beta j\mu}(\Omega). \quad (7)$$

Note that the choice of the HO parameter has no influence in the calculation of the LST since changes to this parameter are equivalent to making a linear transformation in the oscillator variable s. This gives the same result for the right part of Eq. (3).

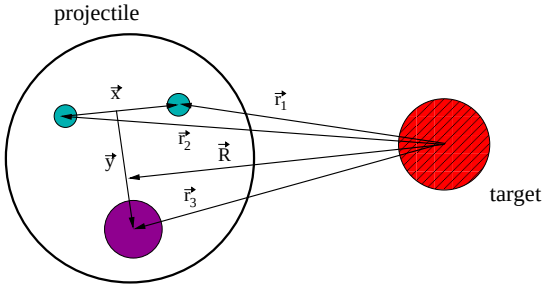

Figure 1: (Color online) Relevant coordinates for the scattering of a three-body projectile by a structureless target.

III. MULTIPOLE EXPANSION OF THE PROJECTILE-TARGET POTENTIAL

The eigenstates given in Eq. (7) are a discrete representation of the states of the three-body projectile. From them, the four-body wavefunction of the projectile-target system, schematically depicted in Fig. 1, is formed as

$$\Psi_{JM}(\boldsymbol{R}, \boldsymbol{x}, \boldsymbol{y}) = \sum_{njJ\mu L M_L} \phi^{THO}_{njJ\mu}(\boldsymbol{x}, \boldsymbol{y}) \langle L M_L j \mu | J M \rangle i^L \times Y_{LM_L}(\widehat{R}) \frac{1}{R} f^J_{Lnj}(R), \quad (8)$$

where $\boldsymbol{R}$ is the coordinate from the target to the center of mass of the projectile, L is the orbital angular momentum of the projectile-target relative motion and J is the total angular momentum, $\boldsymbol{J} = \boldsymbol{L} + \boldsymbol{j}$. The radial functions $f^J_{Lnj}(R)$ satisfy the system of coupled equations

$$\left[-\frac{\hbar^2}{2m_r} \left(\frac{d^2}{dR^2} - \frac{L(L+1)}{R^2} \right) + \varepsilon_{nj} - E \right] f^J_{Lnj}(R) + \sum_{L'n'j'} i^{L'-L} V^J_{Lnj,L'n'j'}(R) f^J_{L'n'j'}(R) = 0, \quad (9)$$

where m_r is the reduced mass of the projectile-target system. The coupling potentials $V^J_{Lnj,L'n'j'}(R)$ are then

$$V^J_{Lnj,L'n'j'}(R) = \langle LnjJM | \widehat{V}_{pt}(\boldsymbol{r}_1, \boldsymbol{r}_2, \boldsymbol{r}_3) | L'n'j'JM \rangle, \quad (10)$$

where the ket $|LnjJM\rangle$ denotes the function $\Phi^{JM}_{Lnj}(\widehat{R}, \boldsymbol{x}, \boldsymbol{y})$ given by

$$\Phi^{JM}_{Lnj}(\widehat{R}, \boldsymbol{x}, \boldsymbol{y}) = \sum_{\mu M_L} \phi^{THO}_{njJ\mu}(\boldsymbol{x}, \boldsymbol{y}) \langle L M_L j \mu | J M \rangle Y_{LM_L}(\widehat{R}). \quad (11)$$

To calculate these coupling potentials, a multipole expansion of the projectile-target interaction is developed. The procedure is analogous to that for a three-body problem reported in Ref. [47]. In that work the traditional method of bin averaging was used as discretization method instead of the THO method. We assume that the projectile-target interaction is the sum of the interactions of each particle of the projectile with the target, $V_{kt}(\boldsymbol{r}_k)$ with $k = 1, 2, 3$. For each pair potential, an appropriate

Jacobi set is chosen so that the corresponding coordinate $\boldsymbol{r}_k$ depends only on the vectors $\boldsymbol{R}$ and $\boldsymbol{y}_k$. Assuming that the potentials are central, the coefficients of the multipole expansion are generated as

$$\mathcal{V}^k_Q(R,y_k) = \frac{1}{2}\int_{-1}^{+1} V^k(r_k) P_Q(z_k) dz_k, \qquad (12)$$

where $P_Q(z_k)$ is a Legendre polynomial, Q is the multipole order and $z_k = \widehat{\boldsymbol{y}}_k \cdot \widehat{\boldsymbol{R}}$ is the cosine of the angle between $\boldsymbol{y}_k$ and $\boldsymbol{R}$. So, the coupling potential can be expressed as

$$V^J_{Lnj,L'n'j'}(R) = \sum_Q (-1)^{J-j}\hat{L}\hat{L}' \begin{pmatrix} L & Q & L' \\ 0 & 0 & 0 \end{pmatrix} W(LL'jj',QJ) F^Q_{nj,n'j'}(R), \qquad (13)$$

where the radial form factor $F^Q_{nj,n'j'}(R)$ is

$$\begin{aligned} F^Q_{nj,n'j'}(R) &= (-1)^{Q+2j-j'}\hat{j}\hat{j}'(2Q+1)\sum_{\beta\beta'}\sum_{k=1}^{3}\sum_{\beta_k\beta'_k} N_{\beta\beta_k}N_{\beta'\beta'_k} \\ &\times (-1)^{l_{xk}+S_{xk}+j'_{abk}-j_{abk}-I_k}\delta_{l_{xk}l'_{xk}}\delta_{S_{xk}S'_{xk}}\hat{l}_{yk}\hat{l}'_{yk}\hat{l}_k\hat{l}'_k\hat{j}_{abk}\hat{j}'_{abk}\begin{pmatrix} l_{yk} & Q & l'_{yk} \\ 0 & 0 & 0 \end{pmatrix} \\ &\times W(l_kl'_kl_{yk}l'_{yk};Ql_{xk})W(j_{abk}j'_{abk}l_kl'_k;QS_{xk})W(jj'j_{abk}j'_{abk};QI_k) \\ &\times \int\int (\sin\alpha_k)^2(\cos\alpha_k)^2 d\alpha_k\ \rho^5 d\rho\ R^{THO}_{n\beta j}(\rho)\varphi^{l_{xk}l_{yk}}_{K_k}(\alpha_k)\mathcal{V}^k_Q(R,y_k)\varphi^{l_{xk}l'_{yk}}_{K'_k}(\alpha_k)R^{THO}_{n'\beta'j'}(\rho), \end{aligned} \qquad (14)$$

with β_k being the set of quantum numbers in the k'th Jacobi system where the potential depends on x_k, and β being the set in the Jacobi system in which the states of the projectile are calculated. The matrix elements $N_{\beta\beta_k}$ transform the hyperangular, angular and spin part of the wave functions from one Jacobi set to another. Their explicit expression as a function of the Raynal-Revai coefficients is developed in Ref. [48]. Note that Eqs. (13) and (14) are completely general, and do not depend on the nature of the basis.

IV. STRUCTURE MODEL FOR ^{6}HE

The ^{6}He nucleus is treated here as a three-body system, comprising an inert α core and two valence neutrons. The ground state has total angular momentum $j^\pi = 0^+$ with experimental binding energy of 0.973 MeV. The ground state wave function was obtained by solving the Schrödinger equation in hyperspherical coordinates, following the procedure described in [25, 48], and making use of the codes FACE [48]+ STURMXX [49]. In these calculations, the n-^{4}He potential was taken from Ref. [50]. It consists of an energy independent Woods-Saxon potential, supplemented by a spin-orbit term with a Woods-Saxon derivative radial shape. This potential reproduces the low-energy s- and p-phase shifts up to 10 MeV. For the NN interaction we used the potential proposed by Gogny, Pires and Tourreil (GPT) [51], which contains central, spin-orbit and tensor components. This interaction was developed to give simultaneously an acceptable fit to two nucleon scattering data up to 300 MeV and to describe reasonably the properties for finite nuclei, particularly the radii, within the Hartree-Fock approximation. Besides the two-body ($n-n$ and $n-\alpha$) potentials, the model Hamiltonian also includes a simple phenomenological three-body force, depending only on the hyperradius, according to the following power form

$$v_{3b}(\rho) = -\frac{a}{1+(\rho/b)^c}, \qquad (15)$$

where a, b, and c are adjustable parameters. This potential is introduced to correct the under-binding caused by our neglect of other configurations, such as the t+t channel.

We have performed different calculations that truncate the maximum hypermomentum at $K_{\max} = 2, 4, 6, 8$, and 10, respectively. For each value of $K_{\max}$, the three-body potential has been adjusted to give the same binding energy and mean square radius (for $j^\pi = 0^+$ states) and the same position for the 2^+ resonance (for $j^\pi = 2^+$ states). The latter value was also used for the $j^\pi = 1^-$ states.

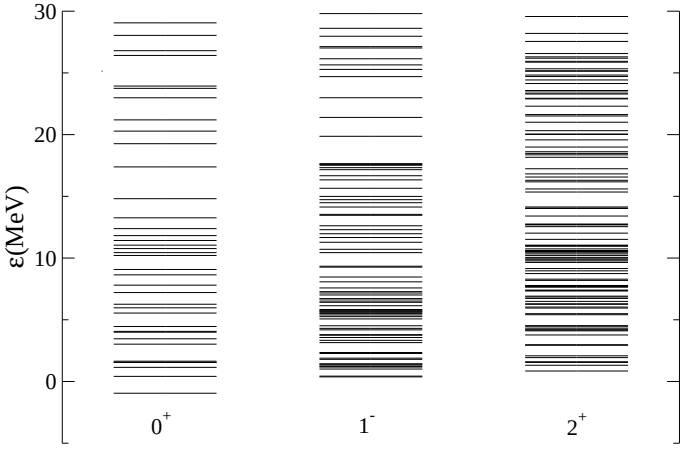

Figure 2: Energy spectrum of the states with $j^\pi = 0^+$, $j^\pi = 1^-$, and $j^\pi = 2^+$ up to 30 MeV excitation, obtained for a THO basis with $K_{\max} = 8$ and $n_b = 4$.

The parameter a varies with $K_{\max}$ and j, being of the order of 4 MeV for $j^\pi = 0^+$ and 3 MeV for $j^\pi = 1^-, 2^+$. The parameter b varies with $K_{\max}$, within the range 4-6 fm. The parameter c was fixed to 3 in all cases.

The number of channels β for each calculation increases drastically with $K_{\max}$, making the calculations much more demanding computationally. In the following, unless stated otherwise, the calculations presented use the basis with $K_{\max} = 8$. As we will show below, this basis provides converged results with respect to the hypermomentum for all the reactions considered in this work. For this case, the number of channels β is 15 for $j^\pi = 0^+$, 26 for $j^\pi = 1^-$ and 46 for $j^\pi = 2^+$. The calculated three-body wave function has a binding energy of 0.95372 MeV and a rms point nucleon matter radius of 2.46 fm when assuming an alpha-particle rms matter radius of 1.47 fm.

The Jacobi set in which the two neutrons are related by the coordinate $\boldsymbol{x}$ is chosen to generate the THO basis. Applying the THO method and diagonalizing the Hamiltonian in a finite THO basis, a set of eigenstates is obtained. For $j = 0^+$, the diagonalization produces a state with negative energy, that corresponds to the ground state of the system. The remaining eigenvalues appear at positive energy, and are then associated with a discrete representation of the continuum spectrum. As an example, in Fig. 2 we present the distribution of eigenvalues obtained for a basis with $n_b = 4$, for the states $j = 0^+$, $j = 1^-$, and $j = 2^+$ up to 30 MeV.

V. APPLICATION TO REACTIONS

In this Section we apply the formalism developed in Sec. III to different reactions induced by ^{6}He, taking the eigenstates obtained with the THO basis to represent the projectile states. We note that, even for a small value of n_b, the THO method will produce eigenstates at very high excitation energies. States above a certain excitation energy will not be relevant for the description of the collision process, since they will be very weakly coupled. For this reason, in these calculations the basis is truncated at a maximum excitation energy, and only those eigenstates below this value were included in the coupled-channels calculation. The maximum energy is chosen independently for each reaction and each n_b, in order to achieve convergence of the results with respect to this energy.

In the present calculations, only the ^{6}He states with $j = 0^+, 1^-, 2^+$ are considered. Previous CDCC calculations for the reactions studied in this work [16, 44, 52] have shown that using these partial waves is sufficient to obtain converged results and to describe satisfactorily the existing data for such reactions. We did not attempt to include higher partial waves, since this would make the calculations very demanding computationally .

For these included j^π states the coupling potentials given by Eq. (13) are calculated for multipolarities $Q = 0, 1, 2$. Both Coulomb and nuclear interactions were included. We emphasize that continuum-continuum couplings were also included. The diagonal as well as non-diagonal coupling potentials were generated by folding the neutron-target and α-target interactions according to Eq. (10). These interactions are represented by phenomenological optical potentials at the relevant projectile incident energy per nucleon [53]. Then, the coupled equations (9) are solved with the code FRESCO [54], that reads the coupling potentials from external files. In most cases, the Numerov method was used to solve the coupled equations. However, in some cases, particularly when excitation energies close to the total kinetic energy are involved, this method was found to be numerically unstable, and the R-matrix method [55] was used instead. This method is more time consuming but has the advantage of being numerically more stable. In the following, we present the results for different reactions for which experimental data exist.

^{6}He+^{12}C. We study this reaction at 229.8 MeV, for comparison with the experimental data of Lapoux et al. [45]. The n+^{12}C potential was taken from the global parametrization of Watson et al. [56]. The α+^{12}C potential was represented in terms of a standard Woods-Saxon shape with the parameters adjusted in order to reproduce the elastic data for this system at 34.75 MeV per nucleon [57]. The parameters for these potentials are listed in Table I.

The coupled equations were solved up to $J = 70$ and the solutions were matched to their asymptotic form at the radius $R_m = 200$ fm. In Fig. 3 we present the angular distribution of the elastic differential cross section relative to Rutherford. The thick solid line is the full CDCC result for a basis with n_b=4. This calculation reproduces the data fairly well (open circles) up to 10°, but it clearly underestimates the data points at larger angles. Interestingly, this effect was also found in the phenomenological analysis of Lapoux et al. [45], as well

Table I: Optical model parameters used in this work. All potentials are parametrized using the usual Woods-Saxon form, with a real volume part and volume (W_v) and surface (W_d) imaginary part. Reduced radii are related to physical radii by $R = r_0 A_T^{1/3}$.

System	V_0 (MeV)	r_0 (fm)	a_0 (fm)	W_v (MeV)	W_d (MeV)	r_i (fm)	a_i (fm)
n+^{12}C	49.46	1.115	0.57	3.05	7.48	1.15	0.5
α+^{12}C	100.	1.289	0.71	19.98		1.738	0.495
n+^{64}Zn	51.82	1.203	0.668	0.29		1.203	0.668
					5.97	1.279	0.534
α+^{64}Zn	123	1.676	0.43	20.40		1.467	0.43
n+^{208}Pb	47.37	1.222	0.726		6.24	1.302	0.351
α+^{208}Pb	96.44	1.376	0.625		32.	1.216	0.42

as in the four-body CDCC calculation of Matsumoto et al. [16] for the same reaction. We also show the analogous calculation when omitting all the couplings to the continuum (one channel calculation) with a dashed line. For the reaction at 229.8 MeV we conclude that the effect of coupling to the continuum is a reduction of the cross section for angles beyond 5°. This effect has also been observed in the scattering of ^{11}Be+^{12}C at $E \simeq 49$ MeV per nucleon [37], and is probably present in other reactions induced by weakly bound projectiles at energies of a few tens of MeV per nucleon. That the no-continuum coupling calculation reproduces the data reasonably well at the larger angles is probably fortuitous, and cannot be attributed to the adequacy of this approximation. As we have shown, continuum couplings are very important in this reaction.

We also show in Fig. 3 the full CDCC calculation for n_b=2 (dotted line). This calculation is practically undistinguishable from the calculation with n_b=4, indicating that it is not necessary in this case to have a very precise discretization of the continuum in terms of excitation energy. We found that a maximum excitation energy of $\varepsilon_{\max}$ =30 MeV provided good convergence for all the values of n_b presented.

^{6}He+^{64}Zn. We have studied this reaction at two different energies, namely, 13.6 MeV and 10 MeV, for which experimental data exist [58]. The n+^{64}Zn potential was taken from the global parametrization of Koning and Delaroche [59]. For the α+^{64}Zn system, we took the optical potential derived in Ref. [58]. The parameters are listed in Table I. The coupled equations were solved up to $J = 60$ and 40, respectively, and for projectile-target separations up to $R_m = 100$ fm.

In Figs. 4 and 5 we present the experimental and calculated angular distributions of the elastic cross section for these two reactions. The dashed lines correspond to the one channel calculations (i.e., omitting the continuum) and the thick solid lines are the full four-body CDCC calculations for a basis with n_b =4.

At $E_{\rm lab}$=13.6 MeV (Fig. 4), the one-channel calculation exhibits a pronounced rainbow peak at around 30°, which is much smaller in the data. Also, this calculation gives a too small cross section at large angles. Inclusion of couplings to the continuum suppresses this rainbow, and enhances the backward angles cross section, improving the agreement with the data in the whole angular range. In the same figure, we also show the full CDCC calculation for a basis with n_b=2 (dotted) and 6 (dot-dashed). These two calculations are very close to n_b=4 showing a very good convergence with respect n_b. The maximum excitation energy required for convergence depended somewhat on the value of nb, ranging from $\varepsilon_{\max}$=7 MeV (for nb=2) to $\varepsilon_{\max}$=6 MeV (for nb=6)

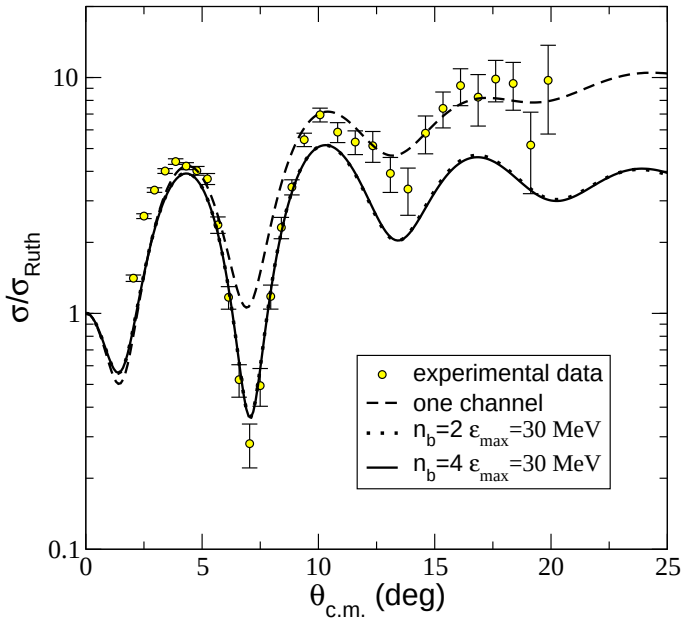

Figure 3: (Color online) Elastic differential cross section relative to Rutherford as a function of the scattering angle in the projectile-target center of mass for the reaction ^{6}He+^{12}C at $E_{\rm lab}$=229.8 MeV. Experimental data are from Ref. [45].

At $E_{\rm lab}$=10 MeV (Fig. 5), the full CDCC calculation also improves the agreement with the data at backward angles, although some underestimation remains. Interestingly, the data suggests the presence of a rainbow at around 50°, which is not present in our calculation. It should be noted that the experimental error bars are large at this energy, so more accurate measurements would be needed to make more definite conclusions about this apparent discrepancy. Again, in the same figure, we show the full CDCC calculation for a basis with n_b=2 (dotted) and 6 (dot-dashed). In this case, we find that the convergence with respect n_b is slower. However the calculations with n_b=4 and 6 are quite close and give a reasonable convergence. As in the previous case, the maximum excitation energy required for convergence depended somewhat on the value of nb, ranging from $\varepsilon_{\max}$=9 MeV (for nb=2) to $\varepsilon_{\max}$=5 MeV (for nb=6).

^{6}He+^{208}Pb. We have performed calculations for this

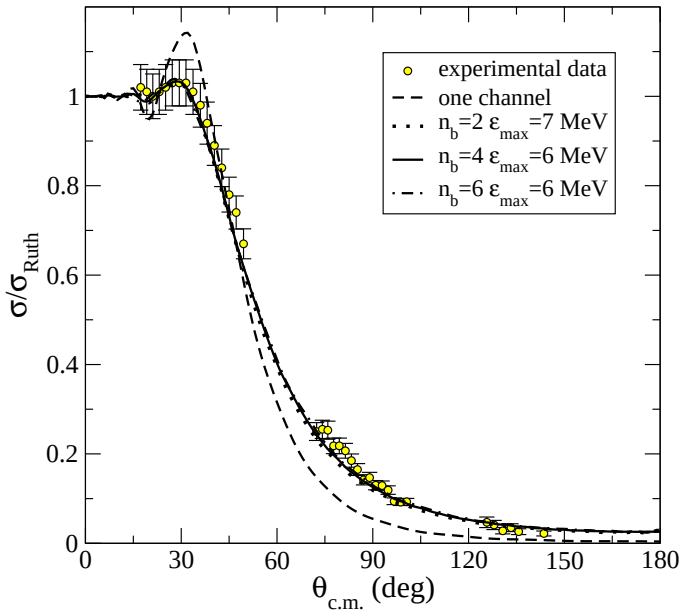

Figure 4: (Color online) Elastic differential cross section relative to Rutherford as a function of the c.m. scattering angle for the reaction ^{6}He+^{64}Zn at $E_{\rm lab}$=13.6 MeV. Experimental data are from Ref. [58].

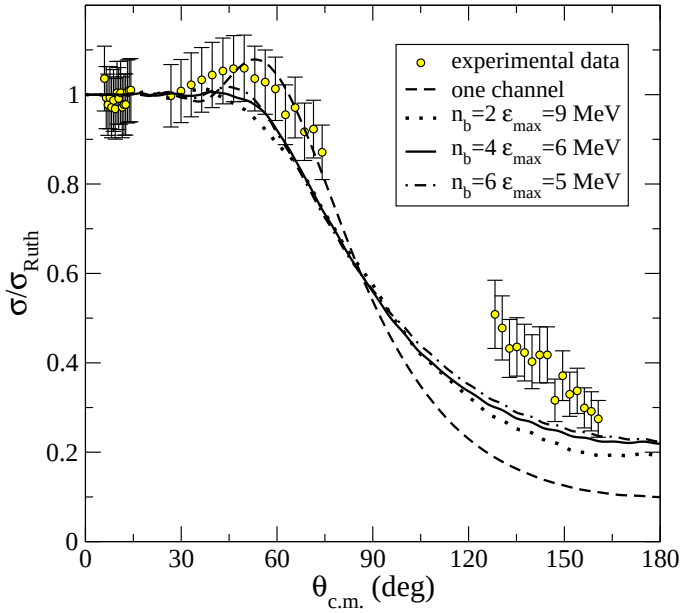

Figure 5: (Color online) Elastic differential cross section relative to Rutherford as a function of the c.m. scattering angle for the reaction ^{6}He+^{64}Zn at $E_{\rm lab}$=10 MeV. Experimental data are from Ref. [58].

reaction at 22 MeV, in order to compare with the recent data of Sánchez-Benítez et al. [60]. We took the n+^{208}Pb potential from Ref. [61] and the α+^{208}Pb potential from Ref. [62]. The parameters for these potentials are also listed in Table I. The coupled equations were solved up to $J = 150$ and matched to their asymptotic solution at

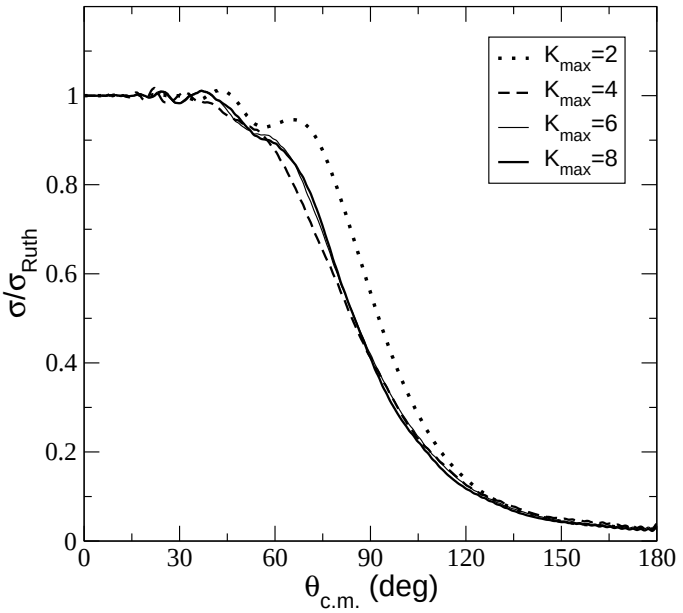

Figure 6: Convergence of the differential elastic cross section with respect to $K_{\rm max}$, for the reaction ^{6}He+^{208}Pb at $E_{\rm lab}$=22 MeV. All the calculations use $n_b = 4$ for the number of hyperradial excitations and the maximum excitation energy was set to 8 MeV.

$R_m = 200$ fm.

First, we discuss the convergence of the calculation with respect the hypermomentum ($K_{\rm max}$) and the hyperradial excitation (n_b). In Fig. 6, we show the calculations with different values of $K_{\rm max} = 2, 4, 6, 8$ and for the same value of n_b=4. For a meaningful comparison, in all these cases the three-body potential was adjusted in order to give the same binding energy and rms radius, for $j = 0^+$ and the same position for the resonance, for $j = 2^+$. We found a relatively fast convergence with respect to this parameter. In particular, the calculations with $K_{\rm max}$ = 6,8 and 10 are very similar (for clarity, the latter has been omitted from the figure). For rest of reactions the results are quite similar, achieving the convergence for $K_{\rm max}$ =6 or 8.

The convergence with respect to n_b for this reaction is illustrated in Fig. 7. For clarity, we show only the results for even values of n_b. Unlike the previous cases, the convergence rate found in this case was rather slow. Although the differences in the calculated cross sections are less than 5%, the oscillatory pattern at the rainbow region changes from one value of n_b to another. A possible explanation for this slow convergence rate is given below.

In Fig. 8 we compare the experimental and calculated angular distributions of the elastic cross section. The dashed line is the one channel calculation and the thick solid line the full CDCC calculation including the continuum. The latter uses $K_{\rm max} = 8$, $\varepsilon_{\rm max} = 8$ MeV, $n_b = 4$. The one channel calculation shows a rainbow that disappears in the full calculation, in agreement with the data.

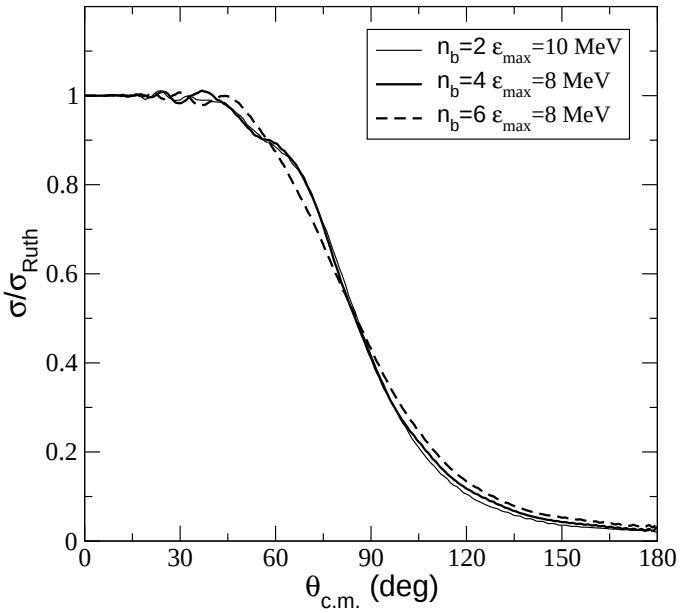

Figure 7: Convergence of the differential elastic cross section with respect to n_b, for the reaction ^{6}He+^{208}Pb at $E_{\rm lab}$=22 MeV.

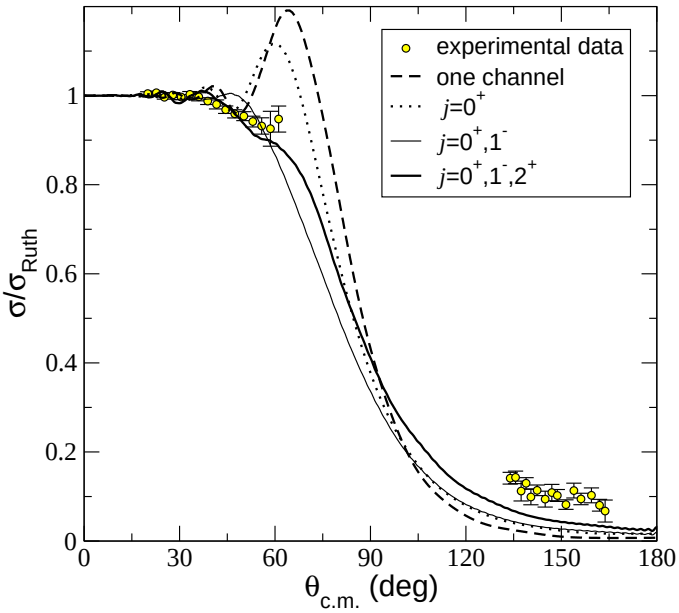

Figure 8: (Color online) Elastic differential cross section relative to Rutherford as a function of the scattering angle in the projectile-target center of mass for the reaction ^{6}He+^{208}Pb at $E_{\rm lab}$=22 MeV. The full CDCC calculations uses n_b =4 and $\varepsilon_{\rm max}$ = 8 MeV. Experimental data are from Ref. [60].

At backward angles, the agreement with the data is improved when we include the coupling to the continuum. In order to show the contribution of the couplings to each j, we also include in this figure the calculation including only $j = 0^+$ states (dotted line) and the calculation with $j = 0^+, 1^-$ states (thin solid line). From these calculations we can conclude that dipole couplings are the main responsible for the characteristic reduction of the cross section at the angles around the rainbow. The strong influence of dipole couplings might explain the slow convergence with respect to the parameter n_b found for this reaction. These couplings are very sensitive to the excitation energy of dipole states, which appear at different positions in our discrete representation of the ^{6}He continuum, as we vary the number of hyperradial excitations, n_b. By contrast, in the ^{6}He+^{12}C case, dipole excitations are very small, and this might explain the fast convergence with respect to n_b in that case.

Moreover, we find that the range of the form factors [Eq. (14)] changes significantly for the different pseudo-states as n_b is changed. This could also contribute to the slow convergence at scattering energies close to the Coulomb barrier.

VI. SUMMARY AND CONCLUSIONS

The collision of a loosely bound three-body projectile with a target nucleus has been studied in the framework of the continuum-discretized coupled-channels (CDCC) method. A set of normalizable states, also known as pseudo-states, is used to represent the three-body continuum of the projectile. In particular we took the Transformed Harmonic Oscillator (THO) basis, which is constructed from the ground state of the system. Within the spirit of the CDCC approach, a multipole expansion of the coupling potentials has been developed for a four-body system (three-body projectile plus a target).

The formalism has been applied to the reactions ^{6}He+^{12}C at 229.8 MeV, ^{6}He+^{64}Zn at 13.6 and 10 MeV, and ^{6}He+^{208}Pb at 22 MeV, taking into account both the Coulomb and nuclear interactions.

Overall, we find good agreement between the calculated and the experimental elastic scattering angular distributions. However, for the ^{6}He+^{12}C reaction at 229.8 MeV the calculations underestimate the experimental data for c.m. scattering angles beyond 10°. The fact that this effect was also found in previous analyses of this reaction [16, 45] suggests that the discrepancy is not related to the particular features of our approach.

For the reaction ^{6}He+^{64}Zn at 13.6 and 10 MeV the calculations are in fair agreement with the data, the reproduction being better in the higher energy case. At 10 MeV our calculations do not predict a rainbow at around 50°, a hint of which is seen in the data, but is broadly consistent with the data within the stated experimental errors.

In actual coupled-channels calculations, the discrete basis has to be truncated in the excitation energy ($\varepsilon_{\rm max}$), the maximum hypermomentum ($K_{\rm max}$), and the maximum number of hyperradial excitations (n_b). In all the cases under study, we have found a good convergence of the calculated observables with respect to the parameters $\varepsilon_{\rm max}$ and $K_{\rm max}$. However, the rate of convergence

with respect to n_b was found to depend very much on the specific reaction. For the reaction ^{6}He+^{12}C at 229.8 MeV the convergence was found to be very fast, with $n_b = 2$ providing fully converged results. For ^{6}He+^{64}Zn at near-barrier energies, we required $n_b \approx 4$ for an acceptable convergence. Finally, for ^{6}He+^{208}Pb at 22 MeV, the convergence was found to be slow and oscillatory. In fact, our biggest calculation, corresponding to $n_b = 6$, is still not fully converged. Because of computational limitations we have not explored this question further, as required to study the convergence of the calculations with respect to the basis size.

This work shows that the use of the transformed harmonic oscillator basis, developed in previous works, combined with the standard CDCC method, provides a reliable procedure for the treatment of the scattering of a loosely bound three-body projectile by a target. It will be interesting to compare this method with other representations of the continuum, including the standard discretization procedure in terms of continuum bins which, in the case of three-body projectiles, requires the calculation of the three-body scattering states. This work is underway and the results will be published elsewhere.

Acknowledgments

This work was supported in part by the DGICYT under projects FIS2005-01105 and FPA 2006-13807-C02-01, and in part by the FCT under the grants POCTI/ISFL/2/275 and POCTI/FIS/43421/2001. This work was performed under the auspices of the U.S. Department of Energy by Lawrence Livermore National Laboratory under Contract DE-AC52-07NA27344. J.A.T. acknowledges the support of the the United Kingdom Science and Technology Facilities Council (STFC) under Grant No. EP/D003628. A.M.M. acknowledges a research grant from the Junta de Andalucía. M.R.G. acknowledges a research grant from the Ministerio de Educación and support from the Marie Curie Training Site program.

[1] K. Riisager, Rev. Mod. Phys. **66**, 1105 (1994).
[2] P. G. Hansen, A. S. Jensen, and B. Jonson, Ann. Rev. Nucl. Part. Sci. **45** , 591 (1995).
[3] A. S. Jensen, K. Riisager, D. V. Fedorov, and E. Garrido, Rev. Mod. Phys. **76**, 215 (2004).
[4] M. Yahiro, Y. Iseri, H. Kameyama, M. Kamimura, and M. Kawai, Prog. Theor. Phys. Suppl. **89**, 32 (1986).
[5] N. Austern, Y. Iseri, M. Kamimura, M. Kawai, G. Rawitscher, and M. Yahiro, Phys. Rep. **154**, 125 (1987).
[6] I. Bray, Comp. Phys. Comm. **85**, 1 (1995).
[7] Z. C. Kuruoglu and F. S. Levin, Phys. Rev. Lett. **48**, 899 (198 ac2).
[8] Z. C. Kuruoglu, Phys. Rev. C **43**, 1061 (1991).
[9] T. Matsumoto *et al.*, Phys. Rev. C **68**, 064607 (2003).
[10] A. Macías, F. Martín, and M. Yáñez, Phys. Rev. A **36**, 4179 (1987).
[11] R. C. Johnson and P. C. Tandy, Nucl. Phys. **A235**, 56 (1974).
[12] B. Anders and A. Lindner, Nucl.Phys. **A296**, 77 (1978).
[13] W. M. Wendler, A. Lindner, and B. Anders, Nucl.Phys. **A349**, 365 (1980).
[14] A. Laid, J. A. Tostevin, and R. C. Johnson, Phys. Rev. C **48**, 1307 (1993).
[15] E. Hiyama, Y. Kino, and M. Kamimura, Prog. Part. Nucl. Phys. **51**, 223 (2003).
[16] T. Matsumoto, E. Hiyama, K. Ogata, Y. Iseri, M. Kamimura, S. Chiba, and M. Yahiro, Phys. Rev. C **70**, 061601(R) (2004).
[17] F. Pérez-Bernal, I. Martel, J. M. Arias, and J. Gómez-Camacho, Phys. Rev. A **63**, 052111 (2001).
[18] F. Pérez-Bernal, I. Martel, J. M. Arias, and J. Gómez-Camacho, Few-Body Syst. Supl. **13**, 217 (2001).
[19] I. Zh. Petkov and M. V. Stoitsov, C. R. Acad. Bulg. Sci. **34**, 1651 (1981).
[20] M. Rodríguez-Gallardo, J. M. Arias, and J. Gómez-Camacho, Phys. Rev. C **69**, 034308 (2004).
[21] A. M. Moro, J. M. Arias, J. Gómez-Camacho, I. Martel, F. Pérez-Bernal, R. Crespo, and F. Nunes, Phys. Rev. C **65**, 011602(R) (2002).
[22] I. Martel, F. Pérez-Bernal, M. Rodríguez-Gallardo, J. M. Arias, and J. Gómez-Camacho, Phys. Rev. A **65**, 052708 (2002).
[23] A. M. Moro, F. Pérez-Bernal, J. M. Arias, and J. Gómez-Camacho, Phys. Rev. C **73**, 044612 (2006).
[24] M. Rodríguez-Gallardo, J. Arias, J. Gómez-Camacho, A. M. Moro, I. J. Thompson, and J. A. Tostevin, Phys. Rev. C **72**, 024007 (2005).
[25] M. V. Zhukov, B. V. Danilin, D. V. Fedorov, J. M. Bang, I. J. Thompson, and J. S. Vaagen, Phys. Rep. **231**, 151 (1993).
[26] I. J. Thompson, B. V. Danilin, V. D. Efros, J. S. Vaagen, J. M. Bang, and M. V. Zhukov, Phys. Rev. C **61**, 024318 (2000).
[27] F. Aksough *et al.*, Review of the University of Milano, Ricerca Scientifica ed educazione permanente **Suppl. 122** (2003).
[28] P. Egelhof, Nucl. Phys. **A722**, C254 (2003).
[29] T. Aumann, L. V. Chulkov, V. N. Pribora, and M. H. Smedberg, Nucl. Phys. **A640**, 24 (1998).
[30] T. Aumann *et al.*, Phys. Rev. C **59**, 1252 (1999).
[31] E. F. Aguilera *et al.*, Phys. Rev. C **63**, 061603(R) (2001).
[32] E. F. Aguilera *et al.*, Phys. Rev. Lett. **84**, 5058 (2000).
[33] O. R. Kakuee *et al.*, Nucl. Phys. **A728**, 339 (2003).
[34] R. J. Glauber, in *Lectures in Theoretical Physics,* Edited by W.E. Brittin (Interscience, New York, 1959), vol. 1, p. 315.
[35] G. D. Alkhazov *et al.*, Phys. Rev. Lett. **78**, 2313 (1997).
[36] J. S. Al-Khalili and J. A. Tostevin, Phys. Rev. C **57**, 1846 (1998).
[37] R. C. Johnson, J. S. Al-Khalili, and J. A. Tostevin, Phys. Rev. Lett. **79**, 2771 (1997).
[38] J. A. Christley, J. S. Al-Khalili, J. A. Tostevin, and R. C. Johnson, Nucl. Phys. **A624**, 275 (1997).
[39] A. K. Kerman, H. McManus, and R. M. Thaler, Ann.

Phys. (N.Y.) **8**, 551 (1959).
[40] K. M. Watson, Phys. Rev. **105**, 1388 (1957).
[41] R. Crespo and R. C. Johnson, Phys. Rev. C **60**, 034007 (1999).
[42] R. Chatterjee, P. Banerjee, and R. Shyam, Nucl. Phys. **A692**, 476 (2001).
[43] S. N. Ershov, B. V. Danilin, J. S. Vaagen, A. A. Korsheninnikov, and I. J. Thompson, Phys. Rev. C **70**, 054608 (2004).
[44] T. Matsumoto, T. Egami, K. Ogata, Y. Iseri, M. Kamimura, and M. Yahiro, Phys. Rev. C **73**, 051602(R) (2006).
[45] V. Lapoux *et al.*, Phys. Rev. C **66**, 034608 (2002).
[46] M. Milin *et al.*, Nuc. Phys. **A730**, 285 (2004).
[47] F. M. Nunes and I. J. Thompson, Phys. Rev. C **59**, 2652 (1999).
[48] I. J. Thompson, F. M. Nunes, and B. V. Danilin, Comput. Phys. Commun. **161**, 87 (2004).
[49] I. J. Thompson, Unpublished. User manual available from the author (2002).
[50] J. Bang and C. Gignoux, Nucl. Phys. **A313**, 119 (1979).
[51] D. Gogny, P. Pires, and R. de Tourreil, Phys. Lett. **B32**, 591 (1970).
[52] A. M. Moro, K. Rusek, J. M. Arias, J. Gómez-Camacho, and M. Rodríguez-Gallardo, Phys. Rev. C **75**, 064607 (2007).
[53] R. C. Johnson and P. J. R. Soper, Nucl. Phys. **A182**, 619 (1972).
[54] I. J. Thompson, Comp. Phys. Rep. **7**, 167 (1988).
[55] A. M. Lane and R. G. Thomas, Rev. Mod. Phys. **30**, 257 (1958).
[56] B. A. Watson, P. P. Singh, and R. E. Seguel, Phys. Rev. **182**, 977 (1969).
[57] S. M. Smith *et al.*, Nucl. Phys. **A207**, 203 (1973).
[58] A. Di Pietro *et al.*, Phys. Rev. C **69**, 044613 (2004).
[59] A. J. Koning and J. P. Delaroche, Nucl. Phys. **A713**, 231 (2003).
[60] A. M. Sánchez-Benítez *et al.*, Nucl. Phys. **A803**, 30 (2008).
[61] M. L. Roberts *et al.*, Phys. Rev. C **44**, 2006 (1991).
[62] A. R. Barnett and J. S. Lilley, Phys. Rev. C. **9**, 2010 (1974).